J. Am. Chem. Soc. **1994,** *116,* 6395–6400

Further Insight in the Surprisingly Complex Unimolecular Fragmentations of the Methyl Nitrite Radical Cation

Detlef Schröder,[*,†] Detlev Sülzle,[‡] Odile Dutuit,[§] Tomas Baer,[*,⊥] and Helmut Schwarz[*,†]

Contribution from the Institut für Organische Chemie der Technischen Universität Berlin, Strasse des 17 Juni 135, D-10623 Berlin, Germany, The Department of Chemistry, University of North Carolina, Chapel Hill, North Carolina 27599-3290, and Laboratoire de Physico Chimie des Rayonnements, URA 75, Bâtiment 350, Université Paris-Sud, F-91405 ORSAY Cedex, France

Received June 25, 1993. Revised Manuscript Received December 16, 1993[●]

Abstract: The unimolecular fragmentation of deuterium and oxygen ^{18}O isotopomers of the methyl nitrite radical cation ($CH_3ONO^{\bullet+}$) was examined by means of tandem mass spectrometry. The [D_1] and [D_2] isotopomers were found to exhibit enormous intramolecular kinetic isotope effects associated with unimolecular $H^\bullet/D^\bullet$ losses. The dissociation rates and breakdown diagrams of energy-selected $CH_3ONO^{\bullet+}$ and $CD_3ONO^{\bullet+}$ ions were measured by photoelectron photoion coincidences. These data exhibit a modest isotope effect. The experimental results imply that the unimolecular $H^\bullet$ and $NO^\bullet$ eliminations occur via a common intermediate, for which we suggest the distonic ion $CH_2O(H)NO^{\bullet+}$. A new ionization energy of 10.44 eV for methyl nitrite is derived. Based on the experimental findings and the results of exploratory *ab initio* MO calculations, two models are presented for the unimolecular dissociation of the methyl nitrite radical cation, in which the initial step involves a 1,2-hydrogen atom migration, $CH_3ONO^{\bullet+} \rightarrow CH_2O(H)NO^{\bullet+}$.

I. Introduction

The unimolecular fragmentation of the metastable methyl nitrate radical cation $CH_3ONO^{\bullet+}$ (**1**) is a long-standing and not fully understood topic in organic mass spectrometry.[1,2] Numerous studies have addressed the reaction mechanism of the fragmentation of **1**,[3] the determination of product ion structures,[4] and the investigation of isomerization processes to other $[CH_3NO_2]^{\bullet+}$ ions.[5] The following conclusions can be drawn. (i) A hydroxymethyl cation, CH_2OH^+, rather than a methoxy cation, CH_3O^+, is formed upon unimolecular $NO^\bullet$ loss from **1** (Scheme 1, reaction I); thus, a hydrogen atom migration precedes and/or accompanies dissociation of **1**. (ii) Reaction I dominates in a relatively narrow energy regime,[2b] which is about 0.3 eV above the ionization energy of CH_3ONO and below the threshold energy for the $CH_3O^\bullet$ loss channel (11.06 eV).[6] The latter process (reaction III) corresponds to a simple O–N bond cleavage in **1** and competes very efficiently with reaction I at energies above 11.06 eV. (iii) Oxygen ^{18}O-labeling experiments exclude the participation of oxygen-atom-equilibrated structures;[3c] similarly, conceivable artifacts due to isobaric interferences in the mass spectrometric experiment were ruled out by high-resolution measurements.[3d] (iv) The photoionization experiments, conducted in two laboratories,[1a,b,7] point to the operation of significant intermolecular deuterium kinetic isotope effects (KIEs) associated with the fragmentation of **1** and its fully deuterated analogue [D_3]**1**. (v) Because the dissociation rate constant as measured by monitoring the appearances of CH_2OH^+ and NO^+ ions differed significantly, Meisels et al.[1a,b] proposed that the reaction was nonstatistical. (vi) The low-energy process leading to a unimolecular $H^\bullet$ loss from **1** (reaction II) has received much less attention, as it has been viewed as just another example of an ordinary, well-understood, single-bond cleavage reaction of organic radical cations.

Scheme 1

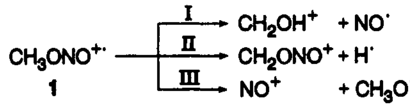

One basic problem associated with the fragmentation process concerns the fact that the efficient competition of reaction III with reaction I requires that the hydrogen migration, preceding or accompanying unimolecular $NO^\bullet$ loss (reaction I), has to occur via a transition structure (TS) located well *below* the threshold for $CH_3O^\bullet$ loss (reaction III).

In the literature, several attempts were reported to explain the slow unimolecular $NO^\bullet$ loss from **1**. In the earliest studies from the Meisels group, surface crossing of excited states of **1** was invoked to rationalize the fragmentation process.[1] Lorquet et al.[2a,3e] applied a predissociative curve-crossing model, which was based on the formation of a deformed methoxy cation with a geometry intermediate between CH_3O^+ and CH_2OH^+. Baer and Hass[3a] suggested the isomerization of **1** to low-energy isomers prior to unimolecular decomposition; however, their arguments were not found to be in keeping with several experimental findings reported by Eggsgaard and Carlsen.[3c] In 1987, Ferguson[3b] proposed the participation of quantum mechanical tunneling in reaction I, and he suggested that $CH_3ONO^{\bullet+}$ first isomerizes to $CH_2ON(H)O^{\bullet+}$. However, this tempting suggestion had to be

---

[†] Technischen Universität Berlin.

[‡] Present address: SCHERING AG, PCS, Müllerstrasse 178, D-13342 Berlin, Germany.

[§] Université Paris-Sud.

[⊥] University of North Carolina.

[●] Abstract published in *Advance ACS Abstracts,* June 1, 1994.

(1) (a) Meisels, G. G.; Hsieh, T.; Gilman J. *J. Chem. Phys.* **1980,** *73,* 1174, 4126. (b) Gilman, J. P.; Hsieh, T.; Meisels, G. G. *J. Chem. Phys.* **1983,** *78,* 3767. (c) Ogden, I. K.; Shaw, N.; Danby, C. J.; Powis, I. *Int. J. Mass Spectrom. Ion Processes* **1983,** *54,* 41.

(2) For discussions and leading references, see: (a) Lorquet, J. C.; Barbier, C.; Leyh-Nihant, B. *Adv. Mass Spectrom.* **1985,** 71. (b) Sirois, M.; Holmes, J. L.; Hop, C. E. C. A. *Org. Mass Spectrom.* **1990,** *25,* 167.

(3) (a) Baer, T.; Hass, J. R. *J. Phys. Chem.* **1986,** *90,* 451. (b) Ferguson, E. E. *Chem. Phys. Lett.* **1987,** *138,* 450. (c) Eggsgaard, H.; Carlsen, L. *Chem. Phys. Lett.* **1988,** *147,* 30. (d) Irion, M. P.; Selinger, A.; Castleman, A. W., Jr.; Ferguson, E. E.; Weil, K. G. *Chem. Phys. Lett.* **1988,** *147,* 33. (e) Leyh-Nihant, B.; Lorquet, J. C. *J. Chem. Phys.* **1988,** *88,* 5606. (f) Egsgaard, H.; Carlsen, L.; Florencio, H.; Drewello, T.; Schwarz, H. *Ber. Bunsenges. Phys. Chem.* **1989,** *93,* 4126.

(4) Burgers, P. C.; Holmes, J. L. *Org. Mass Spectrom.* **1984,** *19,* 452.

(5) (a) For references up to 1989, see ref 2b. (b) Arakawa, R. *Bull. Chem. Soc. Jpn.* **1989,** *62,* 2064. (c) Quian, K.; Shukla, A.; Futrell, J. *J. Am. Chem. Soc.* **1991,** *113,* 7121.

(6) Lias, S. G.; Bartmess, J. E.; Liebman, J. F.; Holmes, J. L.; Levin, R. D.; Mallard, W. G. *J. Phys. Chem. Ref. Data* **1988,** *17,* Suppl. 1.

(7) Some PEPICO data have been presented at the 11th IMSC in Bordeaux, August 29–September 2, 1988.

0002-7863/94/1516-6395$04.50/0

Chart 1

CH_3ONO CH_2DONO CHD_2ONO CD_3ONO $CH_3{}^{18}ONO$

revised as the implications of this 1,3-hydrogen migration mechanism are in conflict with results from high-resolution mass spectrometric measurements.[3d]

Here we present a detailed mass spectrometric study of a new [^{18}O] isotopomer and all possible H/D isotopomers of **1**, i.e., [D_1]**1**, [D_2]**1**, and [D_3]**1** (Chart 1). In contrast to all previous studies, the mixed H/D isotopomers allow the determinatiion of *intra*molecular deuterium kinetic isotope effects. As demonstrated repeatedly, the analysis of *intramolecular* KIEs provides much more mechanistic insight with respect to the understanding of fragmentation processes than analysis of the *intermolecular* variants.[8] In addition, new photoelectron photoion coincidence (PEPICO) data obtained using improved resolution as compared to the previous studies[1] are reported.

II. Experimental Section

The experiments were performed in a modified ZAB/HF/AMD 604 tandem mass spectrometer of BEBE configuration (B stands for magnetic and E for electric sector); this machine and its operation have been described in detail elsewhere.[9] The isotopomeric radical cations of methyl nitrite were generated in an electron impact source (repeller voltage ca. 20 V; electron energy 70 eV) selected by means of B(1)E(1) at a mass resolution of $m/\Delta m \approx 3.000$. Unimolecular fragmentations occurring in the field-free region preceding the second magnet B(2) were monitored by scanning this sector (metastable ion (MI) mass spectrum). Collisional activation (CA) was brought about by colliding the fast-moving ions (8 keV translational energy) with helium (80% transmission); the fourth sector was not used in the present experiments. In order to improve detection statistics and sensitivity for the determination of KIEs associated with $H^\bullet$ and $D^\bullet$ losses, the parent ion regions were scanned separately. Due to the large intensity differences, the linearity of the photomultiplier response was checked by variation of the cascade voltage. The spectra were accumulated and on-line processed either with the VG 11/250 or the AMD-Intectra data system; 5–15 scans were averaged to improve detection statistics and the signal-to-noise ratio. The ratio between $H^\bullet$ and $NO^\bullet$ losses from a given isotopomer depends upon the optimization of the ion optics for these fragments and can very by a factor of ca. 1.5. The data reported refer to an optimization with respect to the hydroxymethyl fragment ion signal ($NO^\bullet$ loss). The reported product ion intensities are the result of averaging at least three separate measurements. The major product ion intensities have experimental errors of <5%.

The PEPICO data were collected at the synchrotron radiation storage ring ACO in Orsay. The experiment and the procedure to extract the rate constants from the PEPICO spectra have been described previously.[10] Briefly, the pulsed light from the ring was dispersed by a 1-m normal incidence monochromator. The photoionization region consisted of a double time-of-flight (TOF) analyzer, one for the electrons, the other for the ions. Threshold electrons with an energy resolution of 10 meV were collected in delayed coincidence with ions. The latter were pulsed out of the ionization region with a 200 V/cm pulse. A two-stage acceleration region and a 14-cm drift region allowed the $H^\bullet$ loss peak to be easily resolved from the parent methyl nitrite ion. The dissociation rates were determined by a previously described method[10b] in which the ions were accelerated by the application of a delayed extraction pulse.

Methyl nitrite isotopomers were prepared at 0 °C from the corresponding labeled methanols[11] (>99 atom % D and >97 atom % ^{18}O, respectively), a saturated aqueous $NaNO_2$ solution, and dilute sulfuric acid (20%); the products were neutralized by condensation on anhydrous K_2CO_3 at −30 °C and purified by distillation. In some experiments, methyl nitrites were generated "*on-line*" in the mass spectrometer as described previously;[2b,3c] identical spectra were obtained using this method. We note, however, that in this experiment the use of PVC tubes may give rise to interference signals due to isobaric $C_2H_4Cl^+$ ions.

III. Results and Discussion

1. Metastable Ion (MI) Decomposition. Table 1 shows the intensities of the various fragment ions produced in the dissociation of metastable isotopomers of **1**. The latter are relatively low in internal energy, with parent ion lifetimes between 20 and 100 μs. The unimolecular dissociations of unlabeled **1** and its isotopomers agree well with previously reported data.[2,3] The $NO^\bullet$ loss (reaction I; $\Delta m = 30$) dominates, whereas reaction III (loss of $CH_3O^\bullet$, $\Delta m - 31$) is of minor importance in the MI time frame. The relatively low intensity of the $H^\bullet$ loss channel, as compared to earlier reports, is due to (i) the absence of artifact peaks in the $[M - 1]^+$ region as a result of mass-selection using double-focusing conditions in our experiments and (ii) a lower internal energy content of metastable **1**. The latter follows from probing metastable ions having a lifetime twice as long as in the previous experiments. Other decompositions of **1** lead to $[M - 2]^{\bullet+}$, $[M - 28]^{\bullet+}$, and $[M - 32]^{\bullet+}$ fragment ions, which will not be discussed in detail. They may be due to some extent to collisions with residual background gas in the field-free region. The most intense of these processes, i.e., the $[M - 32]^+$ fragment, corresponds to loss of $NO^\bullet$ from **1** followed by a consecutive dehydrogenation of CH_2OH^+.[12,13] The fragments formed from the isotopomeric radical cations are in keeping with the previous studies. Whereas unimolecular loss of a neutral methoxy radical, reaction III, is hardly observed in the MI spectra, this process predominates over all other competing reaction channels upon collisional activation (Table 2). The dependency of reaction III on the internal energy content of **1** is in line with a *direct*, continuously endothermic bond cleavage as depicted in Scheme 1.

Surprisingly, the intensity of the unimolecular $H^\bullet$ losses from the radical cations *increases* dramatically upon deuterium incorportion, as evidenced by the MI mass spectra of [D_1]**1** and [D_2]**1**, whereas $D^\bullet$ loss from these precursors is hardly observed (Table 1). After correction for the number of hydrogen/deuterium atoms in the precursor molecules, the *intra*molecular KIEs for the $H^\bullet/D^\bullet$ loss amount to $k_H/k_D = 70 \pm 10$ for [D_1]**1** and $k_H/k_D = 1600 \pm 200$ for [D_2]**1**.[15] While high values for *intra*molecular hydrogen/deuterium KIEs have also been noted previously in unimolecular fragmentations of small metastable organic ions,[16] the most intriguing observation is that the *ratio* of $H^\bullet$ to $NO^\bullet$ losses *increases* with *increasing* deuterium content in [D_1]**1** and [D_2]**1**. If $H^\bullet$ and $NO^\bullet$ losses occurred directly from **1**, deuteration is expected to favor the reaction channel which is not associated with H or D transfer, i.e., reaction I. Our opposite observation indicates that the two channels I and II must be linked with each other (*vide infra*), most likely via a common intermediate. The MI spectrum of the fully labeled isotopomer [D_3]**1** is again similar to that of the unlabeled compound **1**. We note that this finding is another example for the large differences observed in the comparison of *intra-* and *inter*molecular KIEs.[8] As expected, the magnitude of the KIEs is significantly reduced upon collisional activation (Table 2), with $k_H/k_D = 4$ for [D_1]**1** and $k_H/k_D = 12$ for [D_2]**1**.

From the suspected coupling of the $H^\bullet$ and $NO^\bullet$ losses, some conclusions can be drawn with respect to the reaction mechanism

---

(8) Donchi, K. F.; Derrick, P. J. In *Comprehensive Chemical Kinetics*; Bamford, C. H., Tipper, C. F. H., Eds.; Elsevier: Amsterdam, 1983; Vol. 24, p 125.

(9) (a) Srinivas, R.; Sülzle, D.; Weiske, T.; Schwarz, H. *Int. J. Mass Spectrom. Ion Processes* **1991**, *107*, 368. (b) Srinivas, R.; Sülzle, D.; Koch, W.; DePuy, C. H.; Schwarz, H. *J. Am. Chem. Soc.* **1991**, *113*, 5970. (c) Lifshitz, C.; Sandler, P.; Grützmacher, H.-F.; Sun, J.; Weiske, T.; Schwarz, H. *J. Phys. Chem.* **1993**, *97*, 6592.

(10) (a) Richard-Viard, M.; Dutuit, O.; Lavollée, M.; Govers, T.; Guyon, P. M.; Durup, J. *J. Chem. Phys.* **1985**, *82*, 4054. (b) Baer, T.; Dutuit, O.; Mesidagh, H.; Rolando, C. *J. Phys. Chem.* **1988**, *92*, 5674.

(11) Curl, R. F., Jr. *J. Chem. Phys.* **1959**, *30*, 1529.

(12) (a) Hvistendahl, G.; Uggerud, E. *Org. Mass Spectrom.* **1991**, *26*, 67. (b) Uggerud, E.; Helgaker, T. *J. Am. Chem. Soc.* **1992**, *114*, 4265.

(13) The consecutive dehydrogenation of CH_2OH^+, generated unimolecularly from **1**, was verified by a MI/MI experiment (for technical details, see ref 14); it was observed that HCO^+ is formed via the sequence $\mathbf{1} \rightarrow CH_2OH^+ \rightarrow HCO^+$.

(14) Schröder, D.; Schwarz, H. *J. Am. Chem. Soc.* **1990**, *112*, 5947.

(15) The KIE value given for [D_1]**1** represents a lower limit, since the $D^\bullet$ loss channel has some (unknown) contribution from unimolecular H_2 loss from the molecular ion.

(16) (a) Bowen, R. D.; Williams, D. H.; Schwarz, H. *Angew. Chem., Int. Ed. Engl.* **1979**, *18*, 451. (b) For an excellent discussion on the origin of very large kinetic isotope effects, see: Thibblin, A.; Ahlberg, P. *Chem. Soc. Rev.* **1989**, *18*, 209.

Table 1. Mass Differences, Δm (in amu), in the Unimolecular Decomposition (MI) Mass Spectra of the Metastable Methyl Nitrite Radical Cation (**1**) and Its Isotopomers[a,b]

	Δm										
	−1	−2	−3	−4	−28	−30	−31	−32	−33	−34	KIE[c]
1	20	2			2	943	9	24			
[D_1]**1**	172	<1	1		2	777	15	28	4		70 ± 10
[D_2]**1**	532	<1	1	<1	2	440	2	3	18	1	1600 ± 200
[D_3]**1**		10		2	4	867		20		97	
[^{18}O]**1**	18	2				938	<1	34	8		

[a] Data normalized to the sum of all fragment ions with Σ = 1000‰. [b] Some mass differences correspond to combined losses of isobaric neutrals, e.g., Δm = 2 amu from [D_1]**1** accounts for H_2 as well as $D^\bullet$ losses. [c] The kinetic isotope effects (KIEs) refer to the $H^\bullet/D^\bullet$ losses.

Table 2. Mass Differences, Δm (in amu), in the Collisional Activation (CA) Mass Spectra (Helium, 80% Transmission) of Ionized Methyl Nitrate (**1**) and Its Isotopomers[a]

	Δm								
	−1	−2	−30	−31	−32	−33	−34	−35	KIE[b]
1	34		20	100	8	<1			
[D_1]**1**	25	3	18	2	100	4	<1		4
[D_2]**1**	30	5	14	<1	<1	100	<1	<1	12
[D_3]**1**		7	9		1		100	<1	
[^{18}O]**1**	31		19	2	14	100			

[a] Data normalized with respect to the intensity of the base peak being 100%. [b] The KIE values for $H^\bullet/D^\bullet$ losses were somewhat overestimated, since they were not corrected, for metastable ion contributions.

Table 3. Heats of Formation (kcal/mol) of Relevant Species

molecule	$\Delta H_f{}^\circ{}_{298}$	$\Delta H_f{}^\circ{}_0$[a]	ref
CH_3ONO	−15.9	−13.0	*b*
$CH_3ONO^{\bullet+}$	225.0	228.0	this study
$CH_3O^\bullet$	3.7	5.6	*b*
CH_2OH^+	168.0	170.0	*b*
$NO^\bullet$	21.6	21.4	*b*
NO^+	236.0	235.1	*b*

[a] The 0 K values were converted from the 298 K values by using either known or calculated (*ab initio*) vibrational frequencies. [b] Lias, S. G.; Bartmess, J. E.; Liebman, J. F.; Holmes, J. L.; Levin, R. D.; Mallard, W. G. *J. Phys. Chem. Ref. Data* **1988**, *17*, Suppl. 1.

of these processes as well as that of the unimolecular $CH_3O^\bullet$ loss. If we would assume that $H^\bullet$ loss (reaction II) from **1** is a *direct* process, at higher energies one should expect a competition of reaction II with the other direct-bound cleavage process, i.e., reaction III; this has not been observed experimentally. Rather, we suggest that a "hidden"[17] hydrogen migration precedes hydrogen atom loss. The observation of a reverse activation barrier and a kinetic energy release associated with reaction II is in line with this conjecture.[2b]

2. Photoelectron Photoion Coincidence (PEPICO) Study. Table 3 lists the relevant thermochemical information for the various reactions of the methyl nitrite radical cation. Our own threshold photoelectron spectrum of methyl nitrite showed a very weak onset, which is characteristic of ionization processes in which the geometry of the ion and the precursor molecule are very different. While it is difficult to obtain an adiabatic ionization energy (IE_a) from such onsets, the vertical IE_v, which is at the maximum in the Franck–Condon envelope, is readily found to be 10.96 eV. The adiabatic IE was thus determined by combining the measured IE_v with the *ab initio* MO calculations (*vide infra*). The energy of the $CH_3ONO^{\bullet+}$ was calculated using the neutral geometry as well as the fully optimized ion geometry. The difference in these energies of 0.52 eV should be close to the difference in the vertical and adiabatic IEs. This results in IE_a = 10.44 eV, which places the adiabatic IE just at the beginning of the gentle TPES onset. This IE is somewhat higher than the 10.38 eV quoted in the earlier Meisels study.[1b] The reason for this appears to be an incorrect energy scale in the previous study which shifted the TPES and the breakdown diagram to lower energy by about 0.090 eV. Our energy scale was calibrated to the nitric oxide threshold photoelectron spectrum during the course of the experiment.

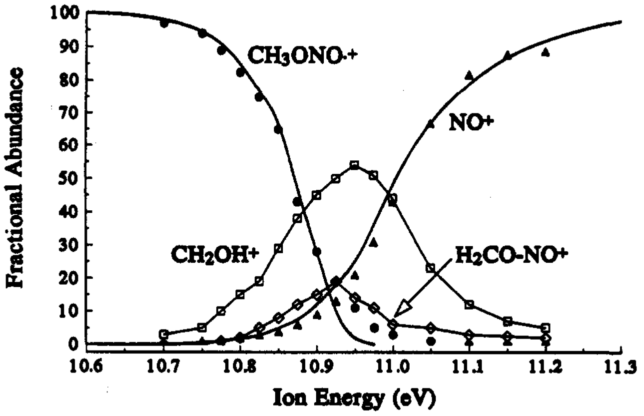

Figure 1. Breakdown diagram for normal methyl nitrite ions obtained from the photoelectron photoion coincidence experiment. The experimental data are shown as points, while the solid lines for the $CH_3ONO^{\bullet+}$ and NO^+ data are calculated using the 0 K breakdown diagram of Figure 3 and the sample's 300 K thermal energy distribution.

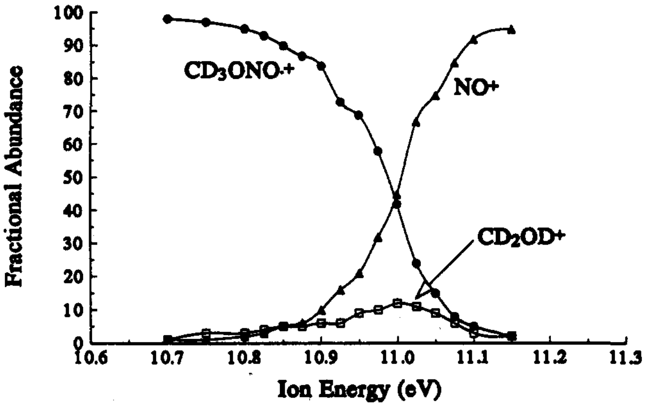

Figure 2. Breakdown diagram for deuterated methyl nitrite ions obtained from the photoelectron photoion coincidence experiment. The $D^\bullet$ loss was too weak to be detected in this study. The solid lines are spline fits through the data.

The breakdown diagrams for the normal and deuterated methyl nitrite ions are shown in Figures 1 and 2. These also differ from the previously reported diagrams of Meisels et al.[1a,b] Firstly, for example, the present results show the $H^\bullet$ loss channel, which was not resolved in the previous work. Secondly, the energy scale in the Meisels $CD_3ONO^{\bullet+}$ breakdown diagram is shifted to lower

---

[17] For this concept, see: Schwarz, H. *Top. Curr. Chem.* **1981**, *97*, 1.

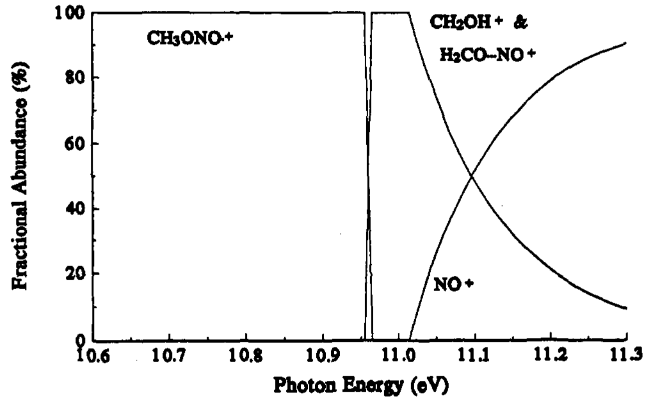

Figure 3. 0 K breakdown diagram of normal methyl nitrite ions. This breakdown diagram, when convoluted with the 300 K thermal energy distribution of methyl nitrite, gives the solid lines in Figure 1.

energy by about 0.09 eV. Of particular interest in the new results is the similar shape of the CH_2OH^+ and H_2CONO^+ signals as a function of the ion internal energy. They rise and fall in nearly the same manner. However, it is apparent that the $H^\bullet$ loss onset is slightly higher than the NO loss onset, so that at very low energies, the NO loss channel dominates. This is the energy region of interest for the metastable ions sampled in the beam experiments (Table 1).

The second interesting feature lies in the comparison of the breakdown graphs of $CH_3ONO^{\bullet+}$ and $CD_3ONO^{\bullet+}$. As noted by Meisels and co-workers,[1a,b] the $NO^\bullet$ loss signal to generate CD_2OD^+ is greatly diminished. What was not obvious in the previous results is the reason for this difference. With the correct energy scales in Figures 1 and 2, it is evident that the rise of the NO^+ signal is identical in the normal and deuterated breakdown diagrams. The major difference is a result of a shift toward higher energy of the parent ion falloff in the $CD_3ONO^{\bullet+}$ dissociation. This "squeezes" the range of energies in which CD_2OD^+ products can be formed.

The breakdown diagrams of Figures 1 and 2 are obtained with a room temperature sample with its thermal internal energy distribution. The average internal energies for room temperature methyl nitrite samples are 87 and 93 meV for the normal and deuterated samples, respectively. This thermal energy distribution has the effect of smearing or broadening the breakdown diagram. By deconvoluting the room temperature breakdown diagram with the thermal energy distribution, it is possible to construct the 0 K breakdown diagram. This is shown for the case of the unlabeled methyl nitrite in Figure 3. The important feature in this 0 K breakdown diagram is the slow rise of the NO^+ signal. It is apparent that the NO^+ and CH_2OH^+ reaction channels are in competition over a considerable energy range. This is, in fact, evident already in the room temperature breakdown diagram (Figure 1), in which the NO^+ signal rises more gently than the parent ion signal drops, a difference that becomes more evident in the constructed 0 K diagram. We will come back to this important fact after discussing the dissociation rates. In addition, we note that the 0 K breakdown diagrams show the onset of NO^+ formation within 5 meV of the thermochemical onset of NO^+ and $CH_3O^\bullet$ production (reaction III). This is in spite of the fact that the NO^+ and $CH_2OH^\bullet$ channel lies 0.4 eV below reaction III and indicates that the latter process cannot compete with the other dissociations (*vide infra*).

In Figure 4, we present the dissociation rates for $CH_3ONO^{\bullet+}$ and $CD_3ONO^{\bullet+}$. These were obtained by analyzing the asymmetric peak shapes in the PEPICO time-of-flight distributions. These rates also differ from those previously reported.[1a,b] The major differences are in the slopes of the $k(E)$ curve. This is especially evident in the case of the deuterated methylnitrite ion rates which were nearly flat in Meisels' data. The more normal $k(E)$ curve in Figure 4, which increases with the internal energy, removes one of the major problems in the interpretation of the previous data.

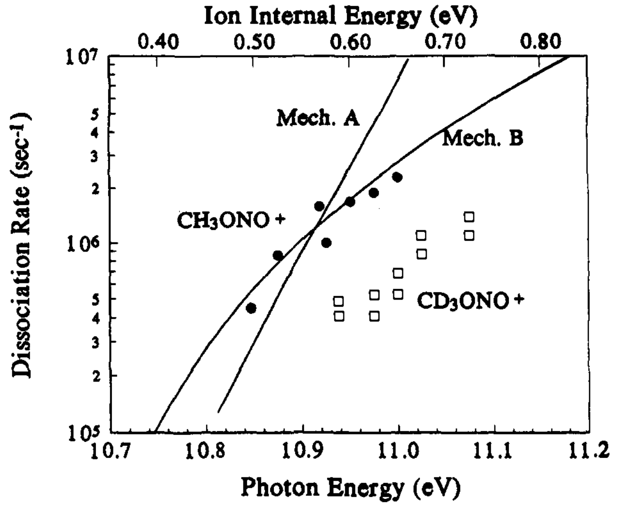

Figure 4. Measured dissociation rates (points) of energy-selected normal and deuterated methyl nitrite ions. The ion internal energy scale is given by: $h\nu - \mathrm{IE} + \langle E_{th} \rangle$, where the IE is the measured ionization energy of 10.44 eV, and $\langle E_{th} \rangle$ is the average internal thermal energy of the methyl nitrite at room temperature. The solid lines are from RRKM calculations and refer to the mechanisms discussed in the text.

IV. *Ab Initio* Molecular Orbital Calculations

In order to understand better the relevant ionic structures in the dissociation of the methyl nitrite radical cation, we carried out some exploratory *ab initio* molecular orbital calculations.[18] Scheme 2 shows the energies of various isomers and transition structures (TS) found using the GAUSSIAN program with the 6-31 G* basis set. Geometrical details of **1**, the central intermediates **2** and **3**, and the transition structure TS **1/2** are given in Chart 2.

In these extensive MO studies, all attempts failed to locate a *low*-energy transition structure connecting **1** with the channels leading to the losses of $NO^\bullet$ and $H^\bullet$.[18-20] The only transition structure found, TS **1/2**, is too high in energy to account for reaction I in terms of a classical trajectory. Furthermore, no TS of any kind could be found connecting isomers **2** and **3**. The fundamental problem appears to be the location of the charge. In isomers **1** and **2**, the charge is largely centered on the nitrogen atom, whereas in **3** and the final product of reaction I, CH_2OH^+, the charge has shifted to the carbon and oxygen atoms. As pointed out by Leyh-Nihant and Lorquet several years ago, this transfer of charge is a result of the intersection of two electronic energy surfaces.[3e] It is for this reason that the NO^+ loss channel is a fast and direct dissociation, while the formation of CH_2OH^+ involves a more circuitous route. While Leyh-Nihant and Lorquet treated reaction I in terms of a curve-crossing between two diabatic electronic surfaces, we instead describe the dissociation in terms of an adiabatic process.

According to Scheme 2, the $H^\bullet$ loss channel produces as the product ion an ion–dipole complex,[21] $[CH_2O\cdots NO^+]$, between the dipolar formaldehyde and the closed-shell NO^+ cation. Its formation is in competition with the loss of neutral $NO^\bullet$. The latter undoubtedly is formed by passing over a barrier which is below the $H^\bullet$ loss asymptote. This is evident from the breakdown

---

(18) (a) Morrow, J. C.; Baer, T., unpublished computational results at the MP4/6-31 G*//6-31G* level of theory. (b) Lehr, H.; Sülzle, D.; Schwarz, H., unpublished computational results at the MP2/6-31G**//MP2/6-31G** level of theory.

(19) We are fully aware that a more reliable theoretical treatment would have to start with a geometry optimization at a CI level. This is presently beyond our technical capabilities.

(20) McKee, M. L. *J. Phys. Chem.* **1986**, *90*, 2335.

(21) McAdoo, D. J. *Mass Spectrom. Rev.* **1988**, *8*, 363.

Scheme 2. Schematic of Part of the Potential Energy Surface of $[CH_3NO_2]^{•+}$ as Calculated by MP4/6-31*//6-31G*[a]

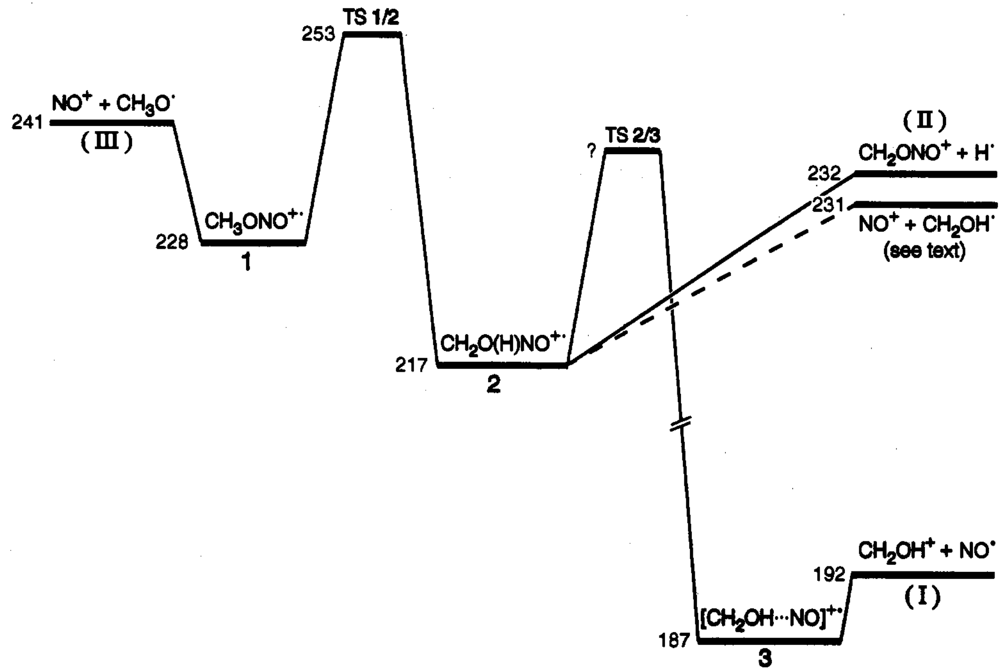

[a] Heats of formation are given in kcal/mol.

Chart 2. Calculated Geometries (6-31G*) of **1**, **2**, **3**, and TS **1/2**[a]

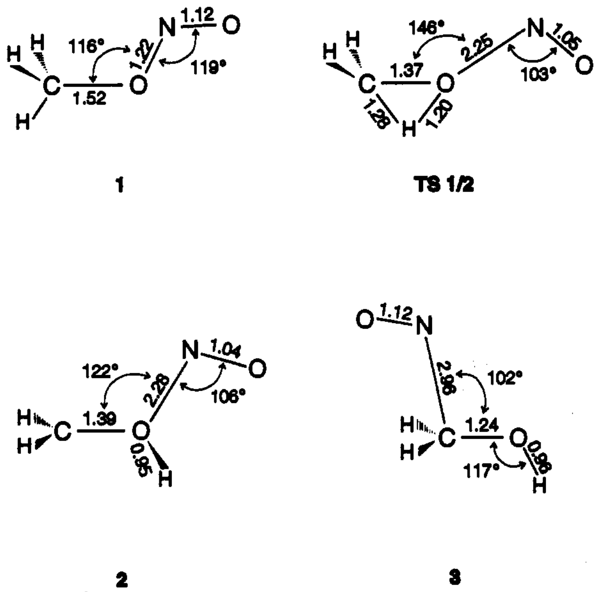

[a] Bond lengths are given in angstroms and bond angles in degrees.

diagram (Figure 1), in which the CH_2OH^+ signal onset is below that of the H• loss signal. The fragment intensities of the metastable ion spectra (Table 1) provide further support. Extrapolation of the dissociation rate to the metastable ion region indicates that the dissociating ions responsible for the fragment intensities have an energy of about 10.7 eV, at which the H• loss channel is nearly eliminated, as observed in the MI spectrum of unlabeled **1**.

An interesting feature in Scheme 2 is that the thermochemical dissociation limit to NO^+ and $CH_2OH^•$ would be isoenergetic with the H• loss channel. Yet neutral $CH_2OH^•$ is apparently not produced, in spite the fact that isomer **2** is ideally suited for its production.[22-24] Apparently, the production of NO^+ from **2** must involve a rearrangement of the CH_2OH group, resulting in a barrier with a minimum height of ca. 0.2 eV. Such a barrier would be sufficient to suppress this channel relative to the H• and NO• losses.

V. Proposed Mechanisms

Our inability to calculate all transition structures connecting isomers **1**, **2**, and **3** prevents us both from definitively determining the rate-limiting step which controls the measured dissociation rates and from interpreting the large intramolecular KIEs in a more quantitative fashion. In particular, we are not yet able to consider the effects of the dissociation dynamics of excited **2** after being formed from metastable **1** on the H•/NO• loss ratio. However, we can offer some qualitative proposals which circumscribe possible future analysis. The potential energy diagram of Scheme 2 suggests two scenarios. In mechanism A, the rate-limiting step corresponds to the H atom transfer via TS **1/2**, while in mechanism II, the barrier associated with TS **2/3** is rate-limiting. In either case, the branching ratio between CH_2OH^+ and NO^+ production is determined by the relative rates of H atom transfer and direct dissociation of **1**.

Mechanism A. According to the *ab initio* calculations, TS **1/2** is about 0.4 eV above the measured onset for NO^+ production. This suggests that the H atom transfer step proceeds via quantum mechanical tunneling. The Eckart potential is a convenient three-parameter function for calculating tunneling probabilities.[25] The parameters required are the *ab initio* calculated imaginary frequency of 2000 cm^{-1} associated with the reaction coordinate, the barrier height, and the reaction endoergicity. These tunneling probabilities can be incorporated into a Rice–Ramsperger–Kassel–Marcus (RRKM) theory calculation as previously de-

---

(22) While there exists evidence in the literature for the cogeneration of two neutral $[CH_3O]^•$ isomers (i.e., the unimolecular decay $CH_3COOCH_3^{•+} \rightarrow CH_3CO^+ + CH_3O^•/CH_2OH^•$ (ref 23)), in the present case there is no compelling evidence for the formation of $CH_2OH^•$ from $CH_3ONO^{•+}$. Actually, the comparison of the MI data for **1** and $[D_3]$**1** is not strongly in favor of a rearrangement preceding NO^+ production. Unfortunately, the analysis of the data of $[D_1]$**1** and $[D_2]$**1** (see Table 1), which indicates an increase of the NO^+ production channel with increasing deuterium content of **1**, a situation reminiscent to the competition of channels I and II (see text), is less straightforward due to isobaric interferences. Experiments aimed at experimentally determining the structure of the $[CH_3O]^•$ radical, for example by using the technique of collision-induced dissociative ionization (ref 24), failed on sensitivity grounds.

(23) Heinrich, N.; Schmidt, J.; Schwarz, H.; Apeloig, Y. *J. Am. Chem. Soc.* **1987**, *109*, 1317 and references cited therein.

(24) Burgers, P. C.; Holmes, J. L.; Mommers, A. A.; Szulejko, J. E.; Terlouw, J. K. *Org. Mass Spectrom.* **1984**, *19*, 442.

(25) (a) Eyring, H.; Walter, J.; Kimball, G. E. *Quantum Chemistry*; Wiley: New York, 1944. (b) Johnston, H. S. *Gas Phase Reaction Rate Theory*; Ronald Press: New York, 1966.

scribed.[26] The rates shown in Figure 4 were obtained when E_0 was assumed to be 7300 cm^{-1}. Although this is lower than the *ab initio* calculated barrier of 1.08 eV (8750 cm^{-1}), it is not unreasonable given the errors associated with *ab initio* calculations of TS as well as those associated with the use of a model function such as the Eckart barrier.

This model can also account for the high intramolecular KIEs. In a tunneling process, hydrogen atom migration will be preferred over the tunneling of a deuterium atom, with the consequence that two isotopomeric distonic ions $CHDO(H)NO^{\bullet+}$ (from [D_1]-**1**) and $CD_2O(H)NO^{\bullet+}$ (from [D_2]**1**) will be formed,[27] hence the large H/D loss ratio. The increased $H^\bullet/NO^\bullet$ loss ratio for the partially deuterated samples has its origin in a more subtle explanation. Substitution of D for H atoms increases the density of vibrational states of isotopomeric **1**, which decreses the rate of isomerization. As a result, the ions sampled in the metastable ion window have a higher internal energy content. In addition, the reduced tunneling probability for partially deuterated **1** also enlarges its internal energy. As already noted in connection with the breakdown diagram, the $H^\bullet$ loss rate rises rapidly at low energies. In fact, statistical dissociation rates increase most rapidly near their threshold. Thus, the effect of partial D atom substitution has the effect of increasing the $H^\bullet$ loss relative to the $NO^\bullet$ loss rates. In addition to this effect, there may be a zero-point energy effect which enhances the KIE. Very likely, a fraction of the metastable nondeuterated methyl nitrite ions have an internal energy below the dissociation limit for $H^\bullet$ loss. However, without a knowledge of accurate vibrational frequencies, this cannot be quantified at present.

Mechanism A suffers from two serious flaws. First, the dissociation rate for the fully deuterated sample is predicted to be considerably slower than the experimentally measured figures. It is slower because (i) the tunneling probability is lower for D atom transfer, (ii) the higher density of states of the deuterated sample slows down the reaction, and (iii) the zero-point energy effect, which raises the activation energy for the deuterated sample. Although precise calculations were not possible for the lack of frequencies for deuterated methylnitrite, we estimate that the shift of the $k_D(E)$ is approximately twice that measured. The second problem with mechanism A is that it predicts a nearly vertical rise of the fractional NO^+ signal in the breakdown diagram. This sudden change arises because, even at the threshold, the NO^+ rate is calculated to be orders of magnitude greater than the $H^\bullet$ atom transfer tunneling rate. It is worthwhile recalling that the Leyh-Nihant and Lorquet[3e] mechanism involving curve-crossing suffers from the same shortcoming.

Mechanism B. This model assumes that the rate-limiting step for $NO^\bullet$ and $H^\bullet$ loss proceeds from the isomerized structure **2**. We thus assume that the TS **1/2** is significantly lower in energy than calculated, so the H atom transfer step, which may still involve quantum mechanical tunneling, is relatively fast. We estimate that its rate constant at an excess energy of 0.3 eV needs to be about 10^7 s^{-1} in order to compete with NO^+ formation at higher internal energies. In this mechanism, isomers **1** and **2** are not equilibrated because the final dissociation step (**2** → products) is faster than the reverse **2** → **1** reaction. The RRKM rate constant for the dissociation of **2** using the calculated energy of isomer **2** is much too high to account for the observed dissociation rates. However, by lowering the energy of isomer **2** by ca. 6 kcal/mol, the dissociation rate is slowed down sufficiently to fall into the experimentally measured range. By assuming that the loosely bound NO^+ and $CH_2OH^\bullet$ entities (note the long O–N bond distance in Chart 2), rotate freely and by assuming a tight TS **2/3**, it is possible to reproduce the measured dissociation rate of unlabeled **1**. The resulting entropy of activation at 1000 K is −13 cal/mol·K. This $k(E)$ curve, labeled as MechB is also shown in Figure 4. Again, deuterated sample rates could not be calculated for lack of frequencies. However, because this reaction does not involve tunneling, the shift of the $k(E)$ curve upon deuteration should be more in line with the experimentally observed shift.

Mechanism B accounts for the high intramolecular KIEs, since it predicts the internal energy of the partially deuterated samples to be just above the onset for $H^\bullet$ loss but below that for $D^\bullet$ loss. Similarly, the high intramolecular KIEs for $H^\bullet/D^\bullet$ losses from small alkanes have been rationalized.[16] Furthermore, mechanism B quite naturally accounts for the slow increase of the NO^+ signal in the breakdown diagram, which is not explained by either tunneling or curve-crossing models.

The major shortcoming of mechanism B is the assumption of a very tight TS **2/3**. $H^\bullet$ loss should involve a rather loose TS (or none). Furthermore, the transfer of the center of charge from the NO to the CH_2OH group is also not expected to involve a particulary tight TS. However, these objections are qualitative in nature.

VI. Conclusions

The intramolecular kinetic isotope effect in the partially deuterated methyl nitrite ion dissociation, the breakdown diagrams for the normal and fully deuterated samples, the dissociation rates, and *ab initio* molecular orbital calculations indicate that $NO^\bullet$ and $H^\bullet$ losses from the methyl nitrite radical cation, **1**, occur via a common intermediate. This intermediate, the distonic ion **2**, is formed via a 1,2-H atom transfer from **1**. In addition, analysis of the breakdown diagram suggests that the reactions which produce NO^+ and CH_2OH^+ ions are in competition over a considerable energy range. Two mechanisms are suggested to explain these findings. One mechanism involves H atom transfer via a rate-determining quantum mechanical tunneling step, while in the second mechanism, the rate-determining step is the dissociation of the distonic ion **2**. A third mechanism is that proposed by Leyh-Nihant and Lorquet, which treats the slow production of CH_2OH^+ in terms of a curve-crossing between two diabatic potential energy surfaces. None of the three models adequately accounts for the data. Neither our mechanism A nor the curve-crossing model is in accord with the finding that NO^+ and CH_2OH^+ are produced with comparable rates over a significant energy range. Mechanism B suffers from somewhat unreasonable assumptions concerning molecular ion and transition-state frequencies. Furthermore, the branching ratio between the $H^\bullet$ and $NO^\bullet$ loss channels may be affected by more subtle effects, e.g., nonstatistical dynamics of rovibrationally excited **2**. A resolution of this problem might be achieved by better absolute and relative rate data with cold samples in order to eliminate the thermal energy distribution. Such data would eliminate the need to deconvolute thermal data and therefore remove any uncertainty concerning the relative rates of NO^+ and CH_2OH^+ formation. In addition, state-of-the-art *ab initio* molecular orbital calculations will be required to resolve this dilemma.

Acknowledgment. Continuous support by the Deutsche Forschungsgemeinschaft and the Fonds der Chemischen Industrie is acknowledged. O.D. and T.B. thank LURE for both financial and technical help in running the synchrotron experiments. T.B. is grateful for financial support from the U.S. Department of Energy and from the National Science Foundation. Dipl.-Chem. *H. Lehr* and Dr. *J. Hrušák* are to be thanked for performing preliminary *ab initio* MO calculations and Professor *P. Ahlberg* for enlightening comments on kinetic isotope effects. Numerous *ab initio* MO calculations of the $[CH_3O_2N]^{\bullet+}$ potential energy surface have been initiated and performed by the late *Professor J. C. Morrow*. Dipl.-Chem. *F. Jeske*, *A. Niklasch*, *A. Nordsieck*, and *W. Zummack* were involved in the synthesis of labeled precursors. We thank all of them for their contributions and the reviewers for constructive criticism.

---

[26] Booze, J. A.; Weitzel, K. A.; Baer, T. *J. Chem. Phys.* **1991**, *94*, 3649.

[27] Jortner, J.; Pullman, B., Eds., *Tunneling*; Reidel: Dordrecht, 1986.